

Article

Magnetism and magnetocrystalline anisotropy of localized 1H/1T by S atom sliding

Eunsung jekal ^{1,†} and Dao Phuong ¹¹ Affiliation 1; Department of Materials, ETH Zurich, 8093 Zurich, Switzerland

* Correspondence:so-young.jekal@mat.ethz.ch

Abstract: Monolayered MoS₂ is energetically most stable when it has a 1H phase, but 1H to 1T phase transition (1H→1T) is easily realized by various ways. Even though magnetic moment is not observed during 1H1T, 0.049 μ_B /MoS₂ is obtained in local 1T phase; 75% 2H and 25% 1T phases are mixed in (2 × 2) supercell. Furthermore, non-negligible magnetocrystalline anisotropy (MCA) energy is occurred. Most magnetic moment as well as MCA are originated by 1T phased Mo atom in the supercell, while electronic structures of other atoms are similar to non-magnetic. Due to this, magnetic/non-magnetic boundary is created in the monolayered MoS₂. Our result suggests that MoS₂ can be applied for spintronics such as a spin transistor.

Keywords: DFT calculation, magnetism, MoS₂

1. Introduction

Recently, research on molybdenum disulfide (MoS₂), which is highly applicable to transistors and solar cells, has been actively conducted[1–6]. MoS₂ has a layered structure similar to that of graphite, but the S-Mo-S bonds in the layer are strong covalent bonds, but the layers and layers are weakly bound by van der Waals interactions, making the layers easily separated [7]. The crystal structures of the bulk Mo₂ are hexagonal symmetry (2H), tetragonal symmetry (1T), and rhombic symmetry (3R). The number before the letter indicates the number of MoS₂ layers contained in the unit cell. The electronic structure of MoS₂ is known to be highly dependent on the symmetry and thickness of the atoms. For example, the 2H phase of the bulk MoS₂ is a semiconductor having a band gap of about 1.2 eV[8], but the 1T phase is a conductor. The shape of the band gap also varies depending on the thickness of the thin film even for the 2H phase[9–11]. It will have an indirect band gap. The biggest advantage of MoS₂ is that it is easy to peel off to a single layer due to the weak interlayer bonding force. In addition, pure MoS₂ does not magnetize regardless of its bulk or thin film thickness, but it can be magnetized in the event of stress, atomic defects, or doping with a small amount of transition metals[9,12,13]. According to the paper, which studies the magnetic and magnetic anisotropy caused by atomic defects, it is observed that about 6% of atomic defects in the single layer MoS₂ generate about 1.989 μ_B of magnetic moment around the defects[14]. In addition, due to the MoS₂ characteristic of the 2H structure, it is possible to have several types of edge structures, such as armchair or zigzag, depending on the cutting direction. In this case, magnetic moments are measured. However, the method of creating defects or edges can lead to unpredictable deformation of the atomic structure and difficult control of the defective molecules and gas molecules adsorbed on the edges. It has been reported that the hydrogen gas is easily adsorbed where the bond is broken and the magnetic moment is greatly reduced when the hydrogen gas is adsorbed.

33 2. Method

34 As a solution to this problem, we focused on experimental papers that create 2H \rightarrow 1T phase
 35 transitions by shifting the position of some S atoms in 2H MoS₂. According to this paper[15], some S
 36 atoms are horizontally shifted along a layer to make some 2H phases transition to 1T phases, thereby
 37 creating a boundary between semiconductors and metals. We have studied the change and magnetism
 38 of the electronic structure in the 1H \rightarrow 1T phase transition in MoS₂. No magnetism was observed when
 39 the entire monolayer was in the 1T phase, but when the 1T phase was locally present in the 1S MoS₂ thin
 40 film, the Mo atoms in the 1T environment were about $0.160 \mu_B$ and the Mo atoms in- the neighboring
 41 1H environment were about $0.011 \mu_B$. It has a chair moment and an average magnetic moment of
 42 $0.049 \mu_B / \text{MoS}_2$. This suggests that, unlike Y.C. Lin and others suggesting a semiconductor/metal
 43 interface by moving some S atoms in a single-layer Mo₂, a magnetic/non-magnetic boundary can be
 44 created. For the purpose of this study, spin-polarized total energy calculations were performed using
 45 the Viennaab-initio simulation (GGA)[16,17] established by Perdew-Burke-Ernzerhof, and pseudo
 46 potentials were generated by the Projector augmented wave (PAW) method. The base cutoff energy
 47 was adopted as a planar wave developed up to 400 eV, and two-dimensional BZ was represented as a
 48 24×24 lattice point of Monkhorst-Pack for the Brillouinzone (BZ) integration[18].

49 In order to perform the film calculation, the distance between the monolayers was sufficiently
 50 given to 15 Å to neglect the interaction between the monolayers and the monolayers. In order to
 51 express a similar situation, the 1H \rightarrow 1T phase transition was implemented by fixing the positions
 52 of the Mo atoms and the lower S atoms and shifting the positions of the upper S atoms collectively.
 53 Fig. As shown in 1 (a), yellow and orange, respectively, were used to distinguish between the lower S
 54 atoms fixed at the upper 1H and the upper S (hereinafter referred to as S') atoms moving to the 1T
 55 phase.

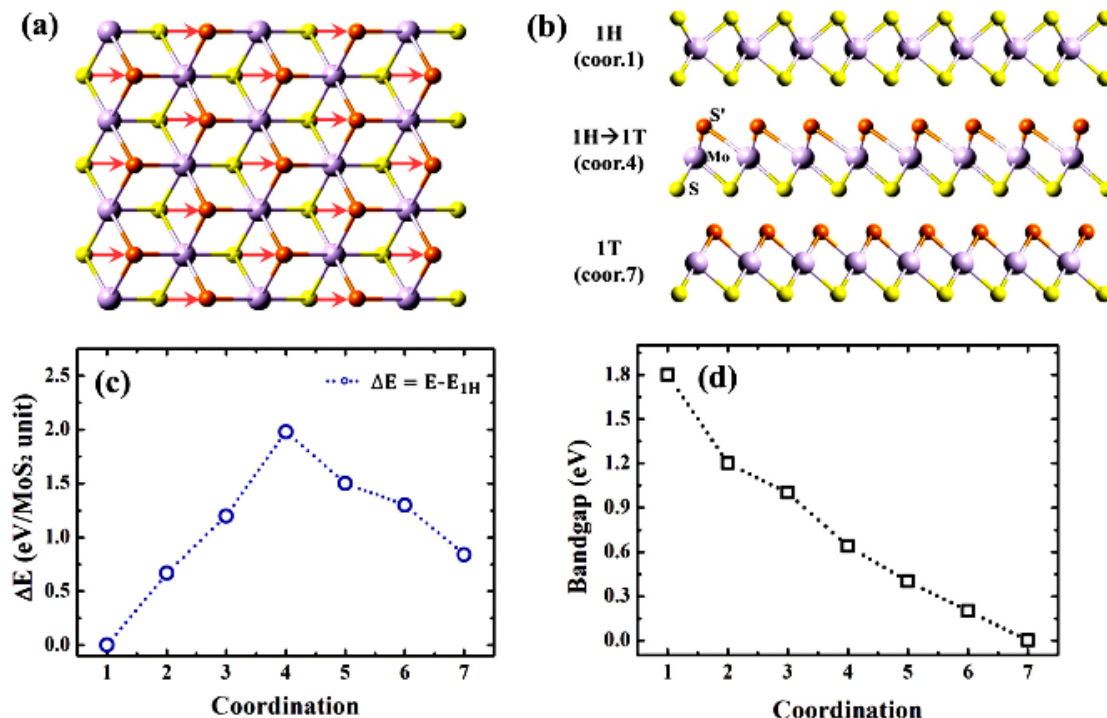


Figure 1. (a) Large sphere represents Mo, small yellow and orange spheres represent S and moved S (S'), respectively. Red arrows express moving path of S' atoms. (b) 1H, center of 1H \rightarrow 1T path and 1T correspond to coord.1, 4 and 7, respectively. (c) Energy difference ($\Delta E = E - E_{1H}$) and (d) band gap on the path of the 1H \rightarrow 1T phase transition.

56 3. Results and discussion

57 To examine the electronic structure in the 1H \rightarrow 1T phase transition intermediate process in a
 58 monolayer MoS₂ thin film. Calculate the energy and band gap at the midpoint of the path indicated by
 59 the arrow in Fig.1 (a). 1(c) and (d), respectively. ΔE of 1 (c) is the total energy calculated based on the
 60 1H phase (E_{1H}). The energy difference between 1H and 1T is approximately 0.84 eV/MoS₂, which is
 61 in good agreement with the results reported earlier. Intermediate of S' path. 4 is calculated to have
 62 about 1.98 eV/MoS₂ higher energy than 1H phase, indicating that the height of the barrier for 1H \rightarrow
 63 1T phase transition is higher than 1.98 eV/MoS₂. Fig. 1 (d) is a change in the band gap on the phase
 64 transition path. The band gap, which is about 1.8 eV at 1H, is steadily narrowed as it approaches 1T,
 65 and the band gap is completely closed at 1T to have a metallic electronic structure. The paramagnetic
 66 states were stable at all points along the path. To account for the local presence of 1T phase in the 1H
 67 phase, set the MoS₂ monolayer (2×2) superlattice and level one-quarter of the number of top S atoms.
 68 The method of moving was chosen. The top and side views of the local 1T structure are shown in Fig.
 69 2 is shown. The dotted lines shown in the top and side views refer to the unit (2×2) superlattice used
 70 in this calculation.

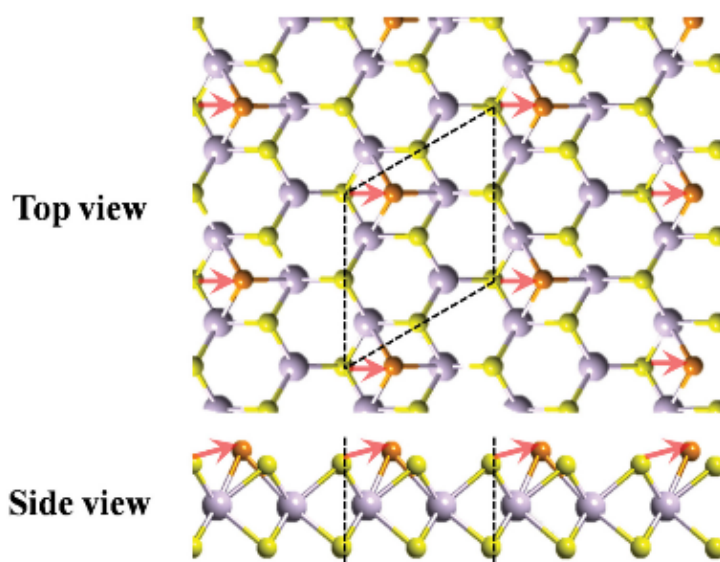


Figure 2. Atomic structure of the local 1T phase MoS₂. Upper (bottom) panel represents top-view (side-view). Dotted lines in both upper and under panels represent the unit cell of the local 1T phase. The moving path of the S' atom is schematically denoted by red arrows.

71 Similar to 1 (a), the S atom immobilized on 1H is yellow and the S' atom that moves to the
 72 1T phase is represented by an orange sphere. The optimal two-dimensional lattice constants were
 73 obtained by loosening the atoms on the z-axis with fixed experimental values for the bulk. The lengths
 74 of Mo-S bonds on the 1H and 1T phases in the local 1T structure were 2.38 Å and 2.44 Å respectively.
 75 The bond length of the 1H portion is reduced compared to that of Mo and S on the pure 1H phase
 76 of 2.41 Å whereas the bond length in the 1T portion is increased. 1H \rightarrow (local 1T) The band gap is
 77 calculated and the results are shown in Fig. 3 (a) and (b). As shown in Fig. 3 (a), the energy difference
 78 between 1H and local 1T is 1.04 eV / MoS₂, which is 0.20 eV/MoS₂ higher than that of the entire 1T
 79 phase. 4 shows that the total energy is higher than about 2.50 eV/MoS₂ 1H phase, and higher
 80 than the 1H \rightarrow 1T energy barrier (1.98 eV/MoS₂), so that the impact of particles with high energy
 81 such as electron beam is required to realize local 1T. Fig. 3 (b) shows the band gap and the magnetic
 82 moment on the movement path of S' simultaneously. The band gap, like the 1H \rightarrow 1T phase transition,
 83 gradually decreases to have a metallic electronic structure even in the local 1T structure.

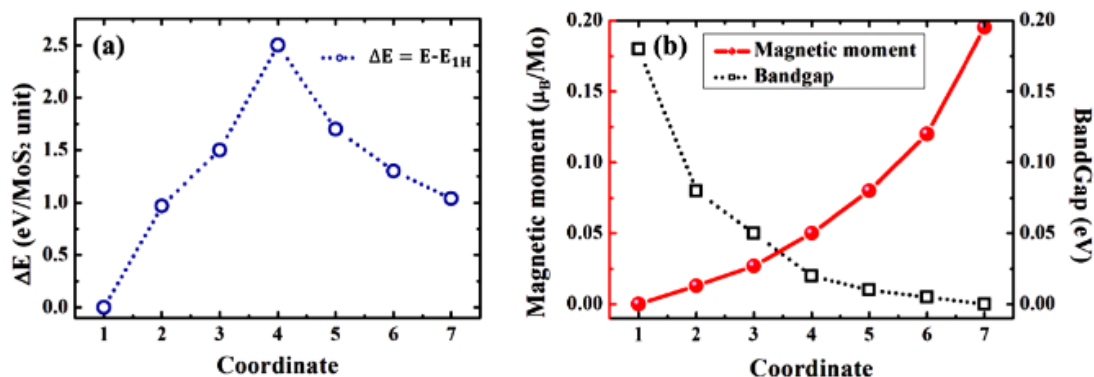


Figure 3. (a) Energy difference ($\Delta E = E - E_{1H}$) and (b) band gap and magnetic moment on the path of the 1H \rightarrow (local 1T) phase transition.

84 On the other hand, in contrast to 1H \rightarrow 1T phase transitions, the magnetic moments of the 1H \rightarrow
 85 (local 1T) phase transitions increased steadily as the S' atoms moved, and the magnetic moments of
 86 about $0.195 \mu_B$ were observed in the fully Korean cattle 1T structure. In order to analyze the Figure 4
 87 shows the spin polarization density of each atom of the local 1T structure. The left figure shows Mo
 88 and S' atoms in the 1T environment within the local 1T, and the right figure shows S closest to the Mo
 89 and S' on the 1H. The contribution of s or p orbits in the state density of Mo is negligible compared
 90 to the contributions of d orbits, so only the d orbits are represented. On the other hand, the S atom
 91 showed only the p orbit because the contribution of the s or d orbit was smaller than the p orbit. As
 92 can be seen from the density of states, most magnetic moments calculated at $0.049 \mu_B/\text{MoS}_2$ are mostly
 93 at 1T Mo atoms. The magnetic moment of the S atoms is negligibly small. Therefore, when considering
 94 the spin polarization density of Mo atoms in the 1T environment, in the energy region below -1.0 eV ,
 95 the state densities of many spins and few spins are almost the same, and the difference is higher only
 96 in the energy region.

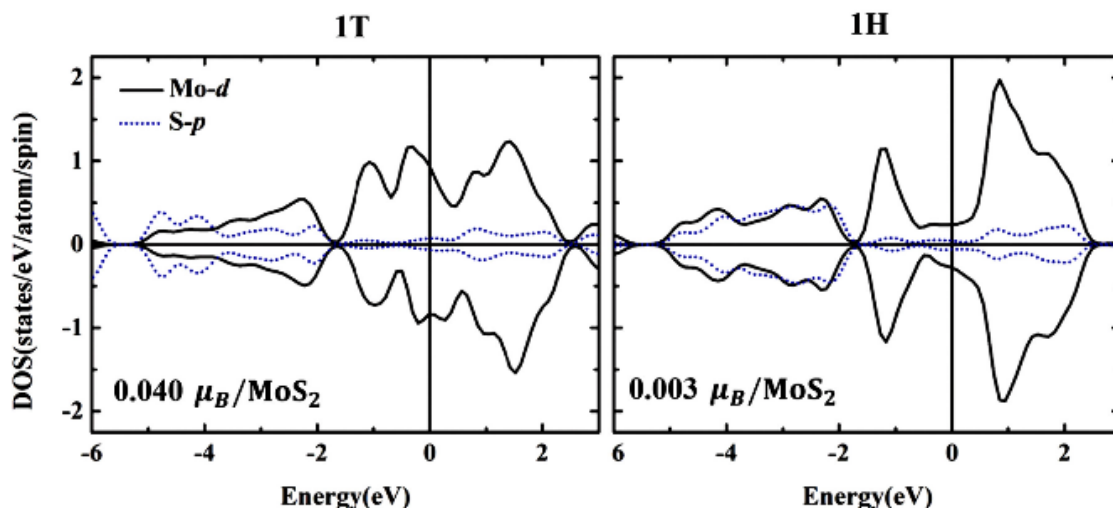


Figure 4. Spin-polarized orbital-projected density of state (DOS) of the local 1T phase MoS_2 . Left panel represents the Mo- d and S' - p orbital in 1T and right panel does the Mo- d and S- p orbital in the nearest neighbor 1H to S' .

97 Further, we also calculated MCA energy through the path path of the 1H \rightarrow (local 1T) phase. On
 98 the 1H phase, there is no MCA energy, however, it sharply increases to 0.14 in coord.5. Then it seems to
 99 be saturated.

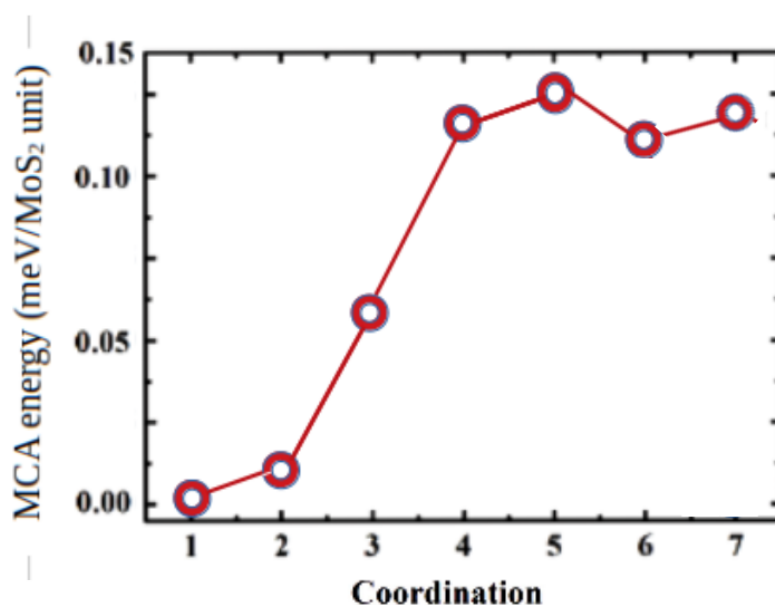


Figure 5. MCA energy on the path of the 1H \rightarrow (local 1T) phase transition.

100 The magnetic moment shown in the local 1T phase is consistent with the previous experimental
 101 and theoretical results of observation of the magnetic moment in MoS₂ with S defects. As such, the
 102 local 1T structure means that a natural magnetic/nonmagnetic boundary can be created, and if used
 103 properly, it can be expected to implement MoS₂-based spintronic devices.

104 4. Conclusion

105 This paper investigates the electronic structure and magnetism of single-layer MoS₂ when phase
 106 transition occurs by using the first principle calculation using VASP. The total energy, band gap, and
 107 magnetism especially MCA energy are examined by setting 1H \rightarrow 1T phase transition and 1H \rightarrow (local
 108 1T) phase transition. The change in the magnetic moment and MCA energy were calculated. As a
 109 result, the barriers of 1H \rightarrow 1T and 1H (local 1T) were quite high, 1.98 and 2.50eV/MoS₂, respectively.
 110 In the 1H phase, the band gap, which was about 1.8 eV, narrowed slightly during the phase transition,
 111 indicating that it had a metallic electronic structure at 1H or 1T. However, unlike 1H \rightarrow 1T, the magnetic
 112 moment as well as magnetocrystalline anisotropy energy were observed in the 1H \rightarrow (local 1T) path,
 113 and if the complete local 1T was calculated to have a magnetic moment of about 0.049 μ_B /MoS₂, Form
 114 DOS, we can know the most of the magnetic moments appeared to contribute to Mo atoms in the
 115 1T environment. Also, 0,14 meV/MoS₂ MCA energy was obtained in the 1H \rightarrow (local 1T) path. The
 116 topical 1T phase is expected to be used as a spintronic device, demonstrating that it is possible to
 117 naturally generate magnetic/nonmagnetic boundaries within a single layer MoS₂.

118 5. Future works

119 5.1. How make $H \rightarrow$ (local 1T) phase transition uniformly in experiment?

120 5.2. Is it same result with Nudged Elastic Band (NEB) calculations?subsection

121 5.3. Why MCA energy occurs and saturates?

122

- 123 1. Ye, G.; Gong, Y.; Lin, J.; Li, B.; He, Y.; Pantelides, S.T.; Zhou, W.; Vajtai, R.; Ajayan, P.M. Defects engineered
124 monolayer MoS₂ for improved hydrogen evolution reaction. *Nano letters* **2016**, *16*, 1097–1103.
- 125 2. Li, L.; Qin, Z.; Ries, L.; Hong, S.; Michel, T.; Yang, J.; Salameh, C.; Bechelany, M.; Miele, P.; Kaplan, D.;
126 others. Role of Sulfur Vacancies and Undercoordinated Mo Regions in MoS₂ Nanosheets Towards the
127 Evolution of Hydrogen. *ACS nano* **2019**.
- 128 3. Jekal, S.; Hong, S.C. First-principles Calculations on Magnetism of 1H/1T Boundary in Monolayered MoS₂
129 **2016**.
- 130 4. Ding, Q. *The Chemistry of MoS₂ and Related Compounds and Their Applications in Electrocatalysis and*
131 *Photoelectrochemistry*; 2016.
- 132 5. Desai, S.B.; Madhvapathy, S.R.; Sachid, A.B.; Llinas, J.P.; Wang, Q.; Ahn, G.H.; Pitner, G.; Kim, M.J.; Bokor,
133 J.; Hu, C.; others. MoS₂ transistors with 1-nanometer gate lengths. *Science* **2016**, *354*, 99–102.
- 134 6. Yun, W.S.; Lee, J. Strain-induced magnetism in single-layer MoS₂: origin and manipulation. *The Journal of*
135 *Physical Chemistry C* **2015**, *119*, 2822–2827.
- 136 7. Cadiz, F.; Tricard, S.; Gay, M.; Lagarde, D.; Wang, G.; Robert, C.; Renucci, P.; Urbaszek, B.; Marie, X. Well
137 separated trion and neutral excitons on superacid treated MoS₂ monolayers. *Applied Physics Letters* **2016**,
138 *108*, 251106.
- 139 8. Zhang, C.; Wang, C.; Rabczuk, T. Thermal conductivity of single-layer MoS₂: A comparative study between
140 1H and 1T phases. *Physica E: Low-dimensional Systems and Nanostructures* **2018**, *103*, 294–299.
- 141 9. Fang, Y.; Hu, X.; Zhao, W.; Pan, J.; Wang, D.; Bu, K.; Mao, Y.; Chu, S.; Liu, P.; Zhai, T.; others. Structural
142 Determination and Nonlinear Optical Properties of New 1T-Type MoS₂ Compound. *Journal of the American*
143 *Chemical Society* **2019**, *141*, 790–793.
- 144 10. Xu, H.; Han, D.; Bao, Y.; Cheng, F.; Ding, Z.; Tan, S.J.; Loh, K.P. Observation of Gap Opening in 1T Phase
145 MoS₂ Nanocrystals. *Nano letters* **2018**, *18*, 5085–5090.
- 146 11. Zhao, W.; Pan, J.; Fang, Y.; Che, X.; Wang, D.; Bu, K.; Huang, F. Metastable MoS₂: crystal structure,
147 electronic band structure, synthetic approach and intriguing physical properties. *Chemistry–A European*
148 *Journal* **2018**, *24*, 15942–15954.
- 149 12. Guo, Y.; Wei, X.; Shu, J.; Liu, B.; Yin, J.; Guan, C.; Han, Y.; Gao, S.; Chen, Q. Charge trapping at the
150 MoS₂-SiO₂ interface and its effects on the characteristics of MoS₂ metal-oxide-semiconductor field effect
151 transistors. *Applied Physics Letters* **2015**, *106*, 103109.
- 152 13. Farmanbar, M.; Brocks, G. Controlling the Schottky barrier at MoS₂/metal contacts by inserting a BN
153 monolayer. *Physical Review B* **2015**, *91*, 161304.
- 154 14. Han, S.W.; Yun, W.S.; Lee, J.; Hwang, Y.; Baik, J.; Shin, H.; Lee, W.G.; Park, Y.S.; Kim, K.S.
155 Hydrogenation-induced atomic stripes on the 2H-MoS₂ surface. *Physical Review B* **2015**, *92*, 241303.
- 156 15. Lin, Y.C.; Dumcenco, D.O.; Huang, Y.S.; Suenaga, K. Atomic mechanism of the semiconducting-to-metallic
157 phase transition in single-layered MoS₂. *Nature nanotechnology* **2014**, *9*, 391.
- 158 16. Sun, G.; Kürti, J.; Rajczyk, P.; Kertesz, M.; Hafner, J.; Kresse, G. Performance of the Vienna ab initio simulation
159 package (VASP) in chemical applications. *Journal of Molecular Structure: THEOCHEM* **2003**, *624*, 37–45.
- 160 17. Hafner, J. Ab-initio simulations of materials using VASP: Density-functional theory and beyond. *Journal of*
161 *computational chemistry* **2008**, *29*, 2044–2078.
- 162 18. Monkhorst, H.J.; Pack, J.D. Special points for Brillouin-zone integrations. *Physical review B* **1976**, *13*, 5188.

